Available online at www.sciencedirect.com

ScienceDirect

JOURNAL OF IRON AND STEEL RESEARCH, INTERNATIONAL. 2016, 23(5): 415-421

Effect of Mg Addition on Nucleation of Intra-granular Acicular Ferrite in Al-killed Low Carbon Steel

Xiao-bing LI, Yi MIN, Zhe YU, Cheng-jun LIU, Mao-fa JIANG

(Key Laboratory for Ecological Metallurgy of Multimetallic Mineral (Ministry of Education), Northeastern University, Shenyang 110819, Liaoning, China)

Abstract: To verify the formation behaviors and mechanisms of intra-granular acicular ferrite (IAF) grains nucleated by Mg-Al-O in low carbon steel, the steels containing different Mg contents were refined in a vacuum induction furnace. The effect of Mg addition on the formation of IAF structure in Al-killed low carbon steel was investigated by optical microscope (OM) and scanning electron microscope with energy dispersive X-ray spectroscope (SEM-EDX). It reveals that the IAFs are only detected in Mg-added steels, and the volume fraction of IAF increases with the Mg concentration from 8×10^{-6} to 26×10^{-6}. It shows that not only the MgO-Al_2O_3-MnS and MgO-Al_2O_3-P_2O_5 particles are the effective nucleation sites for IAF, but also the pure MgO·Al_2O_3 phase can promote the ferrite nucleation. A Mn-depletion zone (MDZ) is characterized adjacent to the MgO-Al_2O_3-MnS, which is believed to be one of the possible mechanisms to explain the IAF nucleation. The MDZ around the MgO-Al_2O_3-MnS inclusion would be induced by the MnS precipitation on the inclusion. It seems that the ability of Mg-containing inclusions to induce the nucleation of ferrite might be attributed to a new mechanism, i.e., the P-rich zone formed on a few Mg-Al-O inclusions might be another factor for promoting the IAF formation.

Key words: low carbon steel; inclusion; magnesium; intra-granular acicular ferrite; Mn-depletion zone

It is generally accepted that intra-granular acicular ferrite (IAF) structure which often nucleates on non-metallic inclusions can refine the austenite grains and improve the toughness of weld metal and/or the heat affected zone (HAZ) of steel weldments[1-5]. In 1900, Mizoguchi and Takamura[6,7] proposed a new concept of oxide metallurgy by utilizing some special non-metallic inclusions to nucleate IAF structure, which finally led to the refinement of the microstructures. Therefore, the oxide metallurgy technology has been widely discussed since then.

Among the various non-metallic inclusions which are considered to be the effective heterogeneous nuclei for IAF during cooling, Ti_xO_y inclusions have been recognized as the most effective nucleation sites for IAF[8-10]. On the other hand, magnesium has even a stronger affinity for oxygen and sulfur than that of titanium. It means that Mg addition can easily distribute fine oxide inclusions in steel, such as MgO, MgO·Ti_xO_y, MgO·Al_2O_3, etc. By comparison, MgO·Ti_xO_y has been considered to be effective sites for ferrite formation by various researchers[11,12]. However, there are still some disagreements on the effects of MgO·Al_2O_3 inclusions on the development of IAF structure. For example, in 2009, Sarma et al.[5] reviewed the role of inclusions in the nucleation of acicular ferrite in steels, and pointed out that MgO·Al_2O_3 was inert for IAF nucleation. However, in 2011, Wen et al.[13] calculated the lattice disregistry among MgO·Al_2O_3 and α-Fe, and found that the value is only 0.6%. Then, they concluded that the MgO·Al_2O_3 can induce the IAF formation according to the lattice mismatch concept proposed by Bramfitt[14]. Regrettably, the pure MgO·Al_2O_3 which induces IAF formation was not detected in the paper, and some other elements, including Mn, S, and Si, coexist with Mg-Al-O in inclusion. Besides, in 2015, Kong et al.[15]

Foundation Item: Item Sponsored by National Natural Science Foundation of China (51374059, 51374060); Scientific Research Fund of Liaoning Provincial Education Department of China (2012221013)

Biography: Xiao-bing LI, Doctor Candidate; **E-mail**: lixb_neu@sina.com; **Received Date**: March 16, 2015

have reconsidered the effect of the Mg-Al-O inclusion on the IAF nucleation, but they still failed to confirm whether the pure $MgO \cdot Al_2O_3$ can promote the IAF formation. In their literature, the associated Mg-Al-O inclusions were chemically homogeneous coexisted with Mn, S, and Si elements. Moreover, they proposed that the magnesium vacancy existed in $MgO \cdot Al_2O_3$, and ascribed the IAF formation mechanism to the Mn-depletion zone (MDZ) around the $MgO \cdot Al_2O_3$ inclusion, which is not consistent with the results of Wen et al.[13]. Above all, the influence of $MgO \cdot Al_2O_3$ on the formation of IAF in steel should be further clarified.

The previous paper[16] has confirmed that Mg addition tended to promote the bainite transformation as a result of the nucleation of acicular ferrite in low carbon steel. But the possible mechanisms of IAF nucleation were not discussed in previous paper. In this study, the formation of IAF structure was further investigated in Mg-Al deoxidized low carbon steel, and another steel with lower Mg content was studied as well. The possible mechanisms of the intra-granular nucleation by Mg-Al-O inclusions were discussed.

1 Experimental Procedure

Three 30 kg ingots of Al-killed low carbon steels were manufactured by a vacuum induction furnace. As Mg has relatively high vapor pressure at steelmaking temperatures, after adding Fe-Al alloy, some Ni-18% Mg alloys were deliberately introduced into the liquid steel with the inside pressure of the furnace at about −0.03 MPa by blowing into the Ar gas. After that, the liquid steel was kept for 1 min and then cast into ingots. Table 1 shows the chemical compositions of the specimens, in which the S1 is the steel with no Mg addition, S2 and S3 are Mg-added steels, and the additions of Mg by using Ni-Mg alloy are 0.024 mass% and 0.072 mass%, respectively.

The obtained ingot specimens were used for inclusion and microstructure observation. The characteristics of inclusions in the specimens with different Mg concentrations were systematically investigated by using scanning electron microscope (SEM, Shinadzu SSX-550TM) equipped with energy dispersive X-ray spectroscope (EDX) and thermodynamic calculations. Microstructure characteristics of the specimens etched by 3 vol. % nital solution were characterized by both optical microscope (OM, ZEISS-Axio Imager M2m) and SEM. Moreover, the mapping scanning analysis and line scanning analysis about the inclusions related with IAF structures were investigated by field-emission transmission microscope (FETM, Ultra Plus, ZEISS) equipped with an EDX.

Table 1 Chemical compositions of experimental steels mass%

Steel	C	Si	Mn	P	S	Ni	Al	Nb	Ti	N	O	Mg
S1	0.05	0.23	1.53	0.009	0.003	0.29	0.03	0.04	0.014	0.0076	0.0037	—
S2	0.05	0.21	1.51	0.008	0.005	0.29	0.03	0.04	0.014	0.0066	0.0041	0.0008
S3	0.05	0.20	1.55	0.008	0.005	0.31	0.03	0.04	0.013	0.0065	0.0040	0.0026

2 Results and Discussion

2.1 Inclusions observation of the steels

The typical inclusions in steels are shown in Fig. 1. Without Mg addition, the detected inclusions are mainly proved to be Al_2O_3-MnS, as shown in Figs. 1(a)—1(d). After adding 8×10^{-6} Mg into the melt, the morphology of the inclusion is similar to that of the S1 sample. However, the central oxide phase is found to be Al-Mg-O and the content of Mg is generally below 10 mass%, which means that the major constituent of the oxide is MgO-depleted magnesia-spinel. After increasing the concentration of Mg to 26×10^{-6}, three types of inclusions are observed: (i) MgO-Al_2O_3-P_2O_5 (-MnS); (ii) MgO-Al_2O_3; (iii) MgO-Al_2O_3-MnS, which are shown in Figs. 1(i)—1(l), respectively. Compared with the S2 sample, the content of Mg is increased to the range of 15 mass%—40 mass%. The ratio of Mg to Al concentration in the central oxide phase is calculated to be about 1∶2 or above this ratio. Then, it is inferred that the central oxide is modified to be magnesia-spinel and MgO-rich magnesia-spinel.

The above-mentioned experimental observations are explained by the thermodynamics of inclusion formation as a function of Mg content, which was calculated using FactSage 6.4 software with the databases of FactPs and FSstel. The phases included in the calculation were liquid, Al_2O_3, MgO, $MgAl_2O_4$, TiO, Ti_2O_3, TiO_2, Ti_3O_5, MnS and MgS. Fig. 2 represents the calculated equilibrium of the thermodynamically stabilized inclusions in samples at a specific

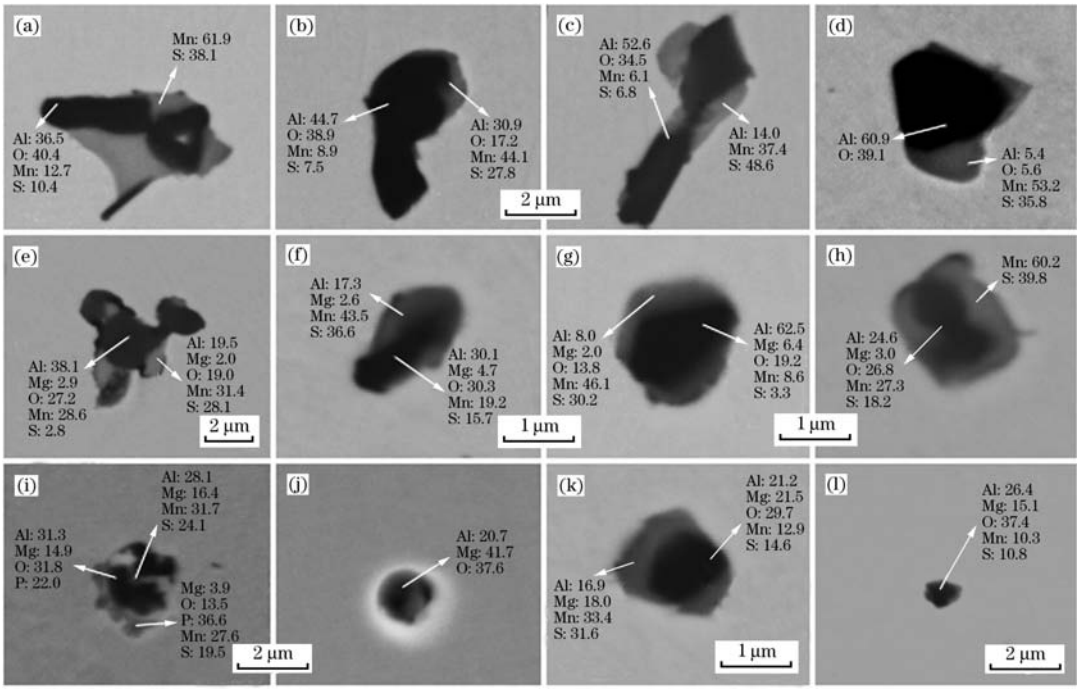

(a)—(d) Inclusions in S1 sample without Mg addition; (e)—(h) Inclusions in S2 sample with low Mg addition; (i)—(l) Inclusions in S3 sample with high Mg addition.

Fig. 1 SEM morphologies and EDX compositions (mass%) of typical inclusions in samples

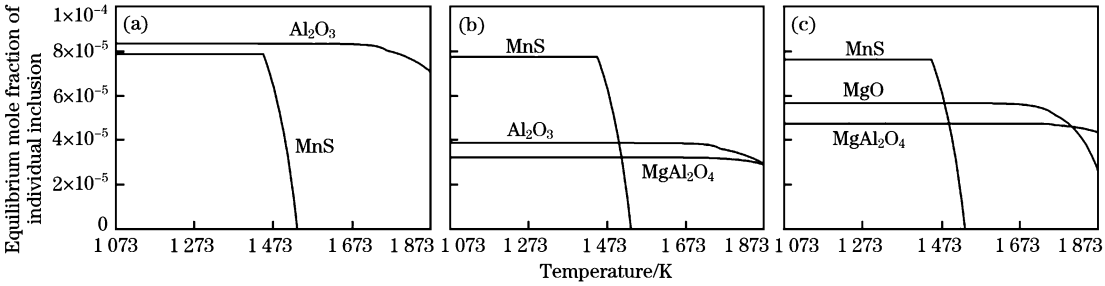

(a) S1; (a) S2; (a) S3.

Fig. 2 Calculated equilibrium of inclusions in samples

temperature of 1873 K. The compositions (mass%) of basic elements used for the calculations were fixed as C 0.05, Mn 1.53, Si 0.20, P 0.008, S 0.005, Al 0.03, Ti 0.014, and O 0.004, which were same as the chemical compositions of the steels. The calculation results confirm that the core oxides are modified with Mg addition, from Al_2O_3 to Al_2O_3-$MgAl_2O_4$ and $MgAl_2O_4$-MgO. It is also revealed by calculation that there is no Ti_xO_y formed in all the steels, and the MnS inclusions are formed during the solidification process. Actually, the results agree well with the experimental observations.

On the other hand, the sizes and total number of the inclusions are also determined quantitatively using SEM, observing sixty-four visual fields of each sample. The size distributions and number density of inclusions in steels are subsequently interpreted with Image Pro Plus 6.0 software, and the results are shown in Fig. 3. It can be found that the size of inclusions in all samples is mainly within 3 μm, and the percentage of inclusions in the range of 0.4—1.5 μm tends to increase for the Mg-added samples. Simultaneously, as can be seen from Fig. 3(b), the number density of inclusions in S2 sample with 8×10^{-6} Mg is similar with that of S1 sample, while it is obviously increased for the S3 sample with 26×10^{-6} Mg. It suggests that moderate Mg addition could contribute to refine the inclusion size and increase the inclusion number density. The differences in the size and the number density of inclusions in three samples might be attributed to the fact that Mg-oxides are not susceptible to growth by collision

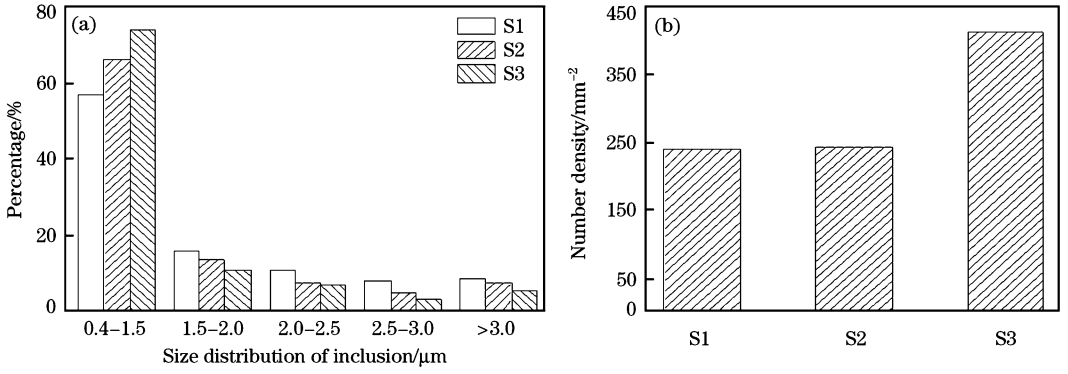

(a) Size distribution; (b) Number density.

Fig. 3 Characteristics of the inclusions in all samples

and agglomeration because they have optimum wettability[11,17-20].

2.2 Microstructures characteristics of the steels

Optical microstructures of the steels are presented in Fig. 4, from which the volume fractions of different microstructures such as polygonal ferrite (PF), pearlite (P) and IAF are characterized as presented in Table 2. The volume fractions of microstructures are determined quantitatively using VNT. Quant-Lab-MG software and observing twenty fields of each steel at a magnification of 200. The IAF structure is determined based on its chaotic arrangement of ferrite plates facing in many different directions within austenite grain[21].

For S1 steel, it consists of large amount of PF and a small proportion of P, but no IAF is detected. The average size of ferrite is nearly 54 μm. After adding

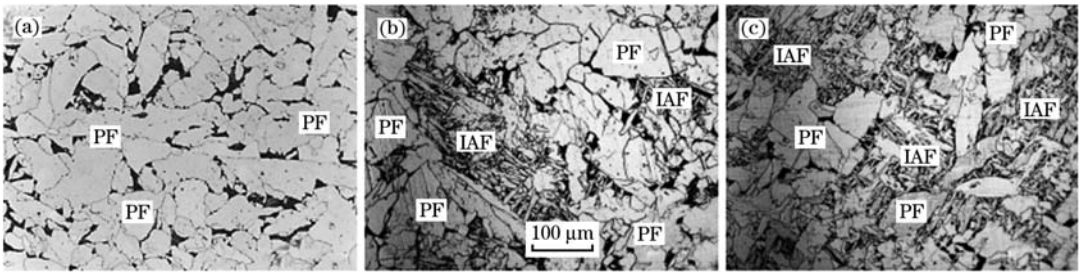

(a) S1; (b) S2; (c) S3.

Fig. 4 Microstructures of experimental steels

Table 2 Volume fractions of PF, P and IAF in steels

Steel	Volume fraction/vol. %		
	PF	P	IAF
S1	91.5±0.90	8.50±0.90	0
S2	90.8±1.20	5.10±1.46	4.12±1.43
S3	83.4±4.80	3.50±0.40	13.1±4.50

Mg into the melts, a certain amount of IAF is observed besides the PF and P phases, as shown in Figs. 4(b) and 4(c). Moreover, the volume fraction of IAF increases intensively with the concentration of Mg from 8×10^{-6} to 26×10^{-6}, and the average size decreases to about 36 μm and 24 μm, respectively. Maybe the inclusions density is not large enough for promoting IAF under the present condition, while the volume fraction of IAF is relatively low as 13 vol. % even in S3 sample. This might restrict the application of the steel when high toughness is quite needed. Nevertheless, the present study indicates that the IAF can be promoted with Mg addition, which would result in the refinement in microstructures.

2.3 Formation behavior and mechanisms of IAF grains from non-metallic inclusions

To account for the IAF existing after adding Mg, the etched microstructure of Mg-added steels were further observed by SEM-EDS, and more than fifty related inclusions were randomly characterized. The typical IAF grains associated with Mg-containing particles in Mg-added steels are shown in Fig. 5.

For S2 steel, it is noted that the $MgO\text{-}Al_2O_3\text{-}MnS$ inclusions can be the effective nucleation of IAF.

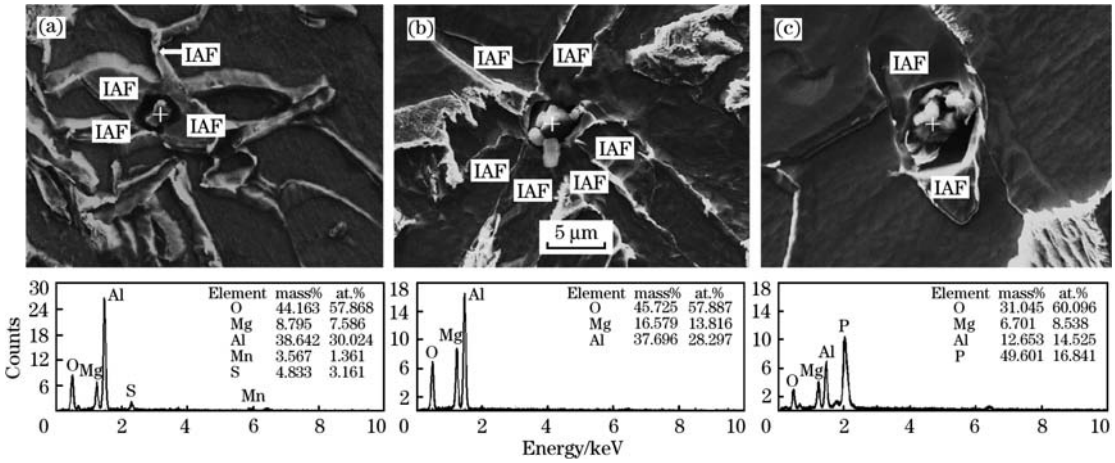

(a) S2; (b), (c) S3.

Fig. 5 SEM micrographs of IAF grains associated with inclusions in steels

According to the results of section 2.1, the dominated inclusions are modified into MgO-Al_2O_3-MnS inclusions for S2 steel. It means that the IAF nucleated in S2 sample is generally due to the inclusions changing from Al_2O_3-MnS to MgO-Al_2O_3-MnS. From the element mapping results (Fig. 6), it is seen that the MnS is being in the outer surface of the oxide inclusion, which is different from the results of Kong et al.[15]. In their literature, the associated Mg-Al-O inclusions are spherical and chemically homogeneous coexisted with Mn, S, and Si elements. In addition, they pointed out that the magnesium vacancy exists in MgO · Al_2O_3 inclusion, and ascribed the MDZ adjacent to the MgO · Al_2O_3 inclusion was induced by the absorption of Mn from steel matrix by MgO · Al_2O_3. However, in fact, it is quite debated that whether there are abundant cation or anion vacancies in MgO · Al_2O_3 or not so far. For example, Wen et al.[13] have explicitly proposed that no cation or anion vacancies are present in MgO · Al_2O_3. Despite this, there has been another viewpoint in regards to the MDZ formation around the specific inclusion besides the cation or anion vacancies mechanism. For instance, Furuhara[22] proposed that MDZ can be induced by the MnS precipitation on Ti_2O_3 during cooling process, and the MnS phase usually locates in outer skin of the oxide inclusion. Moreover, Deng et al.[23] have found that an MDZ is also adjacent to the (Mn-Al-Si-Ti-La-Ce-O)-MnS inclusion, and ascribed this phenomenon to the MnS precipitation on the inclusion.

To confirm the existence of MDZ, the local chemistry distribution, especially for Mn and S, near the specific MgO-Al_2O_3-MnS in S2 steel was further stu-

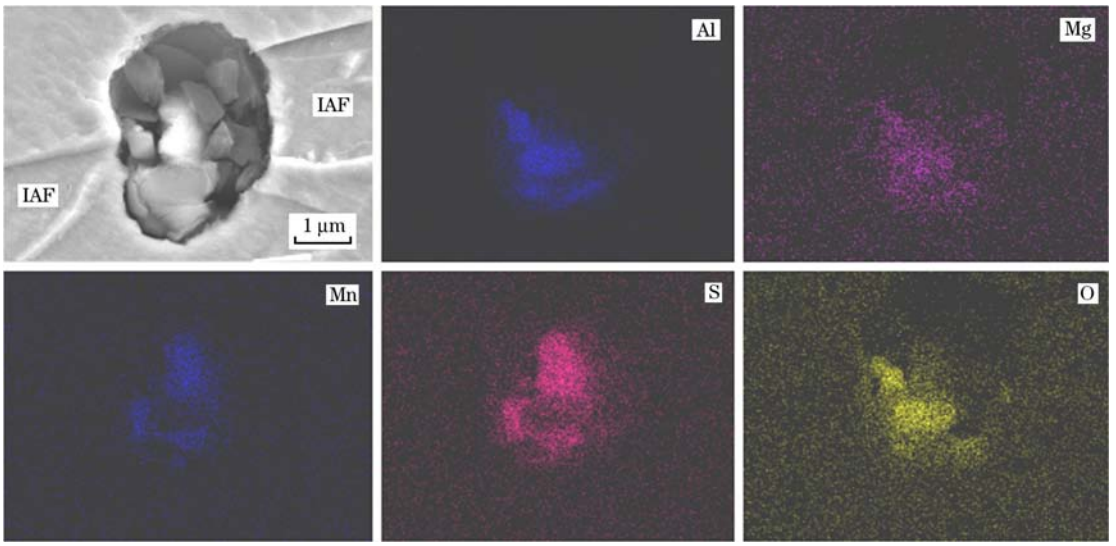

Fig. 6 Element mapping pattern of MgO-Al_2O_3-MnS inclusions nucleating IAF in S2 steel

died, and the results are shown in Fig. 7. It can be seen that a MDZ indeed forms between the steel matrix and MgO-Al_2O_3-MnS. Based on the discussion and thermodynamics calculation, it can be concluded that the MDZ around the MgO-Al_2O_3-MnS inclusion tends to be induced by the MnS precipitation on the oxide inclusion. Thus, the MDZ adjacent to the MgO-Al_2O_3-MnS inclusions would be an important factor for promoting IAF nucleation because Mn is an austenite stabilization element.

For S3 steel, two typical inclusions types associated with IAF were detected. A large proportion of the inclusions is Al_2O_3-MgO, as shown in Fig. 5(b). Moreover, based on the element mapping figure (Fig. 6), it is realized that the inclusion is pure Al_2O_3-MgO phase. It indicates that the pure MgO·Al_2O_3 can indeed induce the IAF formation, which does not agree with the results of Sarma et al.[5]. Furthermore, this could be provided as a further evidence for the theoretical calculation from Wen et al.[13].

In addition, it is seen that the IAF is nucleated on the Al-Mg-P-O inclusion, which is quite different from the previous researches. In fact, Sun et al.[24] have previously proposed MgO-rich inclusions might usually contain a certain amount of phosphorus due to the strong affinity of Mg with P in iron melts. On the other hand, Wen et al.[13] pointed out that a Si enriched zone formed on the MgO-Al_2O_3-SiO_2 inclusion can be one of the possible mechanisms to nucleate the ferrite formation due to that Si is a ferrite element. In this study, it should be noted that several factors are still different from Wen et al.[13], such as the concentration of carbon and silicon elements in steels, both of which are much higher than the present study. Thus, the Si enriched zone accompanied by MgO·Al_2O_3 is not detected, but the Al-Mg-P-O inclusion is detected. It can be inferred that a P-rich zone accompanying with Al-Mg-P-O inclusion would be formed. It is interesting that P is a strong ferrite stabilization element like Si. Then the P-rich zone may also assist the formation of IAF in

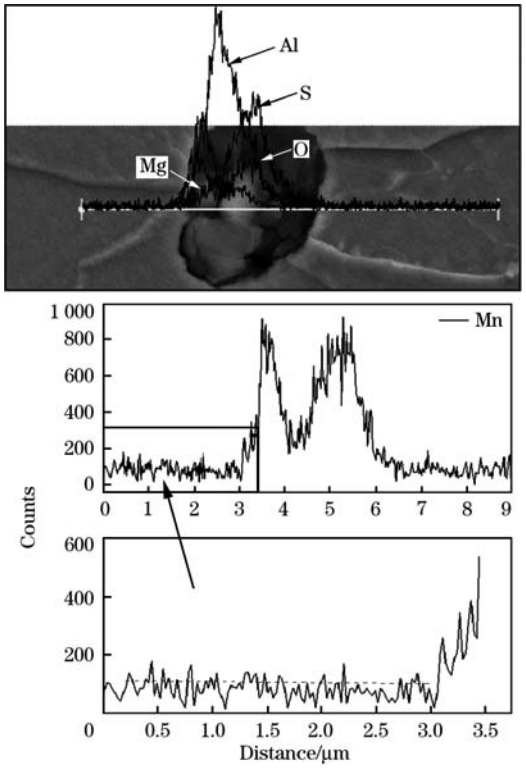

Fig. 7 Line scanning analysis result of typical elements around the MgO-Al_2O_3-MnS inclusions in S2 steel

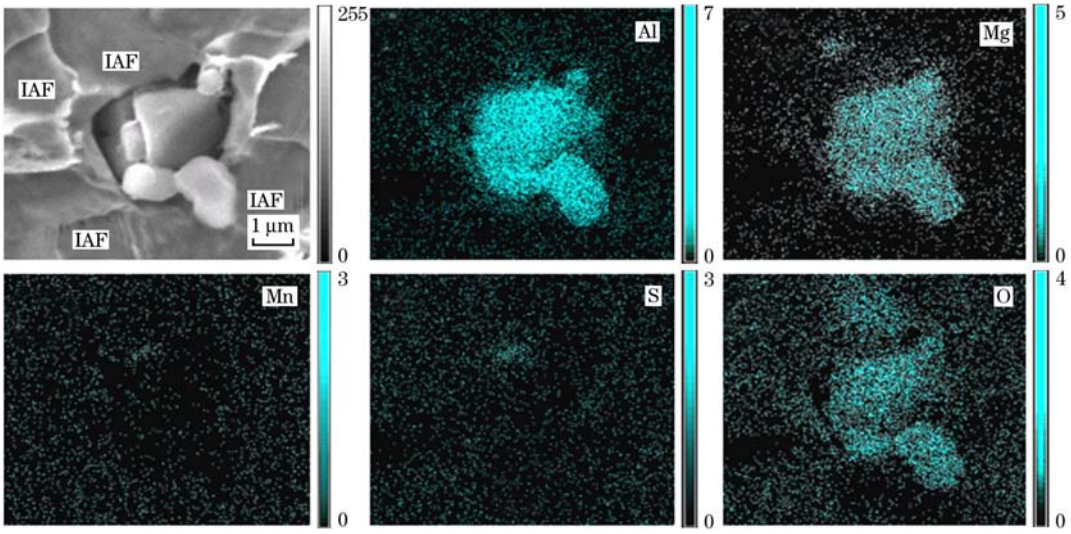

Fig. 8 Element mapping pattern of MgO·Al_2O_3 inclusions nucleating IAF in S3 steel

steel. In fact, Liu et al.[25] have found that phosphorus is frequently observed accompanying with iron sulfide, and they considered that the P-rich zone adjacent to the inclusion might promote the nucleation of acicular ferrite in steel. But they failed to find phosphorus accompanied with oxide inclusion. Moreover, similar results were reported by Umezawa et al.[26] and Yoshida et al.[27] for investigating the effect of phosphorus on the promotion of ferrite nucleation. Unfortunately, as the phosphorus concentration is relatively low as 80×10^{-6} in steel, the number of Al-Mg-P-O inclusions is small. Nevertheless, it is concluded that the Al-Mg-P-O multiphase particles can be nucleation sites for IAF in steel, and the P-rich zone formed on the inclusion might be another factor for promoting the IAF grains formation. Moreover, further investigations are still needed to clarify these phenomena.

3 Conclusions

(1) The IAF structures are promoted by Mg addition, which is mainly due to the dominant oxide inclusions changed from Al_2O_3 to Al_2O_3-MgO, and the volume fraction of IAF structure increases with increasing the concentration of Mg.

(2) It reveals that not only the MgO-Al_2O_3-MnS and MgO-Al_2O_3-P_2O_5 particles can be the effective nucleation of ferrite, but also the pure $MgO\cdot Al_2O_3$ phase can promote the ferrite nucleation.

(3) A MDZ is characterized adjacent to the MgO-Al_2O_3-MnS, which is believed to be one of the possible mechanisms to nucleate the IAF formation. It can be concluded that the MDZ around the MgO-Al_2O_3-MnS inclusion would be induced by the MnS precipitation on the inclusion. It seems that the ability of Mg-containing inclusions to induce IAF might be attributed to a new mechanism, i. e. , the P-rich zone formed on a few Mg-Al-O inclusions might be another factor for promoting the IAF formation.

References:

[1] T. Koseki, G. Thewlis, Mater. Sci. Technol. 21 (2005) 867-879.

[2] Y. Smith, A. P. Coldren, R. L. Cryderman, Toward Improved Ductility and Toughness, Climax Molybdenum Co., Ltd., Tokyo, 1972.

[3] A. H. Koukabi, T. H. North, H. B. Bell, Met. Construction 7 (1979) 639-648.

[4] P. L. Harrison, R. L. Farrar, J. Mater. Sci. 16 (1981) 2218-2226.

[5] D. S. Sarma, A. V. Karasev, P. G. Jonsson, ISIJ Int. 49 (2009) 1063-1074.

[6] S. Mizoguchi, J. Takamura, in: Proc. 6th Int. Iron Steel Cong., ISIJ, Nagoya, 1990, pp. 2331-2342.

[7] J. Takamura, S. Mizoguchi, in: Proc. 6th Int. Iron Steel Cong., ISIJ, Tokyo, 1990, pp. 591-597.

[8] J. H. Shim, Y. W. Cho, S. H. Chung, J. D. Shim, D. N. Lee, Acta Mater. 47 (1999) 2751-2760.

[9] J. S. Byun, J. H. Shim, Y. W. Cho, D. N. Lee, Acta Mater. 51 (2003) 1593-1606.

[10] H. H. Jin, J. H. Shim, Y. W. Cho, H. C. Lee, ISIJ Int. 43 (2003) 1111-1113.

[11] H. S. Kim, C. H. Chang, H. G. Lee, Scripta Mater. 53 (2005) 1253-1258.

[12] F. Chai, C. F. Yang, H. Su, Y. Q. Zhang, Z. Xu, J. Iron. Steel Res. Int. 16 (2009) No. 1, 69-74.

[13] B. Wen, B. Song, N. Pan, Q. Y. Hu, J. H. Mao, Ironmak. Steelmak. 38 (2011) 577-683.

[14] B. L. Bramfitt, Metall. Mater. Trans. 1 (1970) 1987-1995.

[15] H. Kong, Y. H. Zhou, H. Lin, Y. J. Xia, J. Li, Q. Yue, Z. Y. Cai, Advances in Mater. Sci. Eng. (2015), Article ID 378678, http://dx. doi. org/10. 1155/2015/378678, in press.

[16] X. B. Li, Y. Min, C. J. Liu, M. F. Jiang, Steel Res. Int. 86 (2015) 1530-1540.

[17] S. Kimura, K. Nakajima, S. Mizoguchi, Metall. Mater. Trans. B 32 (2001) 79-85.

[18] H. Ohta, H. Suito, ISIJ Int. 46 (2006) 14-21.

[19] J. Yang, T. Yamasaki, M. Kuwabara, ISIJ Int. 47 (2007) 699-708.

[20] R. Takata, J. Yang, M. Kuwabara, ISIJ Int. 47 (2007) 1379-1386.

[21] G. I. Rees, H. K. D. H. Bhadeshia, Mater. Sci. Technol. 10 (1994) 353-358.

[22] T. Furuhara, CAMP-ISIJ 11 (1998) 1129-1132.

[23] X. X. Deng, M. Jiang, X. H. Wang, Acta Metall. Sin. (Engl. Lett.) 25 (2012) 241-248.

[24] W. S. Sun, G. R. Ding, J. Fu, Y. G. Yu, A. R. Wang, Ordnance Mater. Sci. Eng. 20 (1997) 3-8.

[25] Z. Z. Liu, Y. Kobayashi, F. Yin, M. Kuwabara, K. Nagai, ISIJ Int. 47 (2007) 1781-1788.

[26] O. Umezawa, K. Hirata, K. Nagai, Mater. Trans. 44 (2003) 1266-1270.

[27] N. Yoshida, O. Umezawa, K. Nagai, ISIJ Int. 43 (2003) 348-357.